THERMAL PERFORMANCE OF STAGGERED BARE TUBE BANK HEAT EXCHANGER AS AIR PRE-HEATER FOR SEAWEED CONVECTIVE DRYER

Jehuda Marcoveej Titahelu[1)*], Cendy S E Tupamahu[2)], Benjamin G Tentua[3)], Sefnath J E Sarwuna[4)], Antoni Simanjuntak[5)], Nicolas Titahelu[6)]

[1)]S1 Teknik Mesin Fakultas Teknik Universitas Pattimura, Ambon 97234
[1*]ehudatitahelu09@gmail.com
[2,3,4,5,6)]Jurusan Teknik Mesin Fakultas Teknik Universitas Pattimura, Ambon 97234
[2]tupamahucendy@gmail.com [3]golfintentua@gmail.com [4]etwansarwuna19@gmail.com
[5]antonisimanjuntak4@gmail.com [6]titahelunick@gmail.com

Abstrak Pemanfaatan energi limbah panas pengering dengan suhu keluar < 55 C melalui penukar kalor tube bank bare staggered sebagai pemanas awal udara untuk pengeringan rumput laut. Penelitian bertujuan untuk mendapatkan kecepatan udara efektif dimana kinerja termal maksimum dan suhu udara keluar penukar kalor. Metode penelitian eksperimental dengan memvariasikan kecepatan udara 0,5 hingga 2,5 m/s pada ST, SL, D dan L konstan. Pengambilan data terukur kecepatan udara bebas, suhu fluida dingin, dan suhu fluida panas setelah sistem mencapai keadaan tunak. Hasil penelitian menunjukkan bahwa semakin meningkat kecepatan udara bebas maka semakin besar pula kinerja termal dan koefisien konveksi masing-masing sebesar 38,77% dan 38,05% pada kecepatan udara bebas maksimum. Sebaliknya semakin besar kecepatan udara bebas maka suhu keluar akan semakin menurun sebesar 99,60%, dimana suhu udara keluar maksimum berada pada kecepatan udara bebas 2,5 m/s sebesar 303,6 K atau kenaikan sebesar 1,9 derajat. Disimpulkan bahwa sebaiknya penukar kalor ini beroperasi pada kecepatan udara bebas 1,0 m/s guna menjaga keseimbangan kinerja termal dan suhu udara keluar.

Kata kunci: Penukar kalor tube bank, tata letak staggered bare tube, kinerja termal, pemanas awal udara, suhu udara keluar

Abstract *Utilization of drying waste heat energy with an outlet temperature < 55 ℃ through a bare staggered tube bank heat exchanger as an air preheater for drying seaweed. The research aims to obtain the effective air velocity at maximum thermal performance and the heat exchanger exit air temperature. Experimental research method by varying the air velocity from 0.5 to 2.5 m/s at constant* S_T, S_L, *D, and L. Retrieval of measured data on free air velocity, cold fluid temperature, and hot fluid temperature after the system reaches a steady state. The research results show that the greater the free air speed, the greater the thermal performance and convection coefficient, respectively 38.77% and 38.05% at maximum free air velocity. On the other hand, the greater the free air velocity, the more the exit temperature will decrease by 99.60%, where the maximum exit air temperature is at a free air velocity of 2.5 m/s of 303.6 K or an increase of 1.9 degrees. It was concluded that this heat exchanger should operate at a free air velocity of 1.0 m/s to maintain a balance in thermal performance and exit air temperature.*

Keywords: Tube bank heat exchanger, staggered bare tube layout, thermal performance, air preheater, outlet air temperature.

Penulis korespondensi, HP: +62 82251560730
Email: ehudatitahelu09@gmail.com

1. INTRODUCTION

Energy is required for several practical functions, including transportation [1–3], mobility [4], food preparation [5], water purification [6], communication [7], and others [8]. Population and global economic expansion have contributed to increased energy use over time, with end-use energy efficiency gradually increasing with technological advances and energy efficiency legislation. However, this increase is not always enough to offset the rise in demand for energy services, such as commodity production and consumption [9]. In addition, the ongoing conflict between Russia and Ukraine has caused an energy crisis that has directly affected households' heating, cooling, and transportation energy costs [10].

The challenges due to energy shortages and environmental pollution are increasing [11]. This is mainly caused by the lack of fossil fuel reserves, unbalanced energy supply, air contamination, global warming, climate change, acid rain, and ozone damage in the stratosphere [12–16]. Therefore, all countries worldwide are starting to rely on existing resources to become a sustainable 'green' development pattern [17], limiting fuel oil quality and price and controlling pollutant emissions [18]. To anticipate the energy crisis and control pollutants, various efforts have been made to design and optimize energy systems focused on finding new energy sources or increasing efficiency [19]. Increase the use of renewable energy, such as solar energy [20–23], biomass energy [24–28], wind energy [29], geothermal energy [30–32], ocean current energy [33] dan hydrocarbon energy [34–36]. to meet household needs, heating, cooling and transportation. One way to increase efficiency and prevent energy loss is by recycling energy, namely diverting energy wasted as waste heat into the consumption cycle using a heat exchanger [37–44]. The use of a bare staggered tube bank heat exchanger in this study is expected to save electrical energy and reduce waste heat temperature before it is discharged into the environment. This will reduce global warming and global energy consumption.

The heat produced in fuel combustion or chemical reactions that are no longer utilized effectively is called 'waste heat' and is ultimately discharged into the environment [45–47]. Waste heat recovery approaches can be converted into other proper forms of energy without additional electrical energy [48], and is considered an effective measure for a sustainable eco-friendly development mode in various industries [49]. Facts show that more than 50% of the energy used is wasted as waste heat that can be used as an energy source [47], [50], [51]. Waste heat recovery energy conservation technology equipment, one of which is a heat exchange [47], where the type of heat exchanger is a plate heat exchanger [52–55], tube bank heat exchanger [56–61], shell and helical coil heat exchangers [62–69], shell and tube heat exchangers [70–73], dan shell and serpentine tube heat exchangers [74–78].

The heat exchanger is a device designed for efficient heat transfer from one medium to another, where the media are separated by a wall so that they do not mix [79]. A tube bank heat exchanger is a cross-flow tubular heat exchanger consisting of several rows of tubes, where hot fluid flows internally in the tube. In contrast, cold fluid flows externally outside the tube, so heat exchange occurs in cross-flow over the tube [80]. Crossflow tube bank heat exchangers are used in many applications, such as the power industry, biomedicine, air cooling systems (economizers and evaporators), polymer processing, and biological systems [81]. The thermal performance of a tube bank heat exchanger is influenced by geometric parameters, namely tube pitch (L) [82], tube size, transverse pitch tube (S_T), longitudinal pitch tube (S_L), tube length (H) [83], tube configuration (in-line and staggered) [84]. Flow parameters include Reynolds number (Re), air flow speed (u_e) [85] and fluid parameters namely Prandtl number (Pr), friction force (f) and pressure drop (ΔP) [57, 86].

Generally, convective drying suffers from various disadvantages, such as long processing times and high energy costs [87]. Existing industrial drying techniques consume 20-25% of the total energy supplied [88–91], while around 30-40% of the energy is wasted -waste into the environment as waste heat [92–94], where the temperature of waste heat from convective dryers is usually < 55 °C [95]. The problem of energy waste can be overcome if energy-saving strategies are implemented to recover waste heat in the exhaust airflow of the dryer [96]. Tube bank heat exchangers as waste heat recovery systems can reduce fuel waste and global warming [47]. Furthermore, the temperature of the hot air that comes out will be used to heat the cold air to reduce fuel consumption and lower the waste heat temperature through a bare staggered tube bank heat exchanger, which is applied for the convective drying process.

Various studies have been carried out regarding bare staggered bank tube heat exchangers, including evaluating the volumetric density of heat transfer from circular and elliptical configurations of staggered external flow from bare and fin tube banks. It turns out that the relative heat transfer reaches 80% at a speed of 10.0 m/s or Re = 10,600 with a three-way elliptical configuration (S/2b, e, ϕ_f) [97]; a numerical study evaluated the heat transfer speed of circular and elliptical bare staggered configurations, external flow, by varying the air velocity 0.1, 0.13, 0.3, 0.65 m/s, experimentally. It turns out that the relative heat transfer reaches 20% with an equilateral triangle elliptical configuration (S/2b, e, ϕ_f) [98]; the thermal-hydraulic performance study was evaluated by considering the effects on the heat transfer rate and pressure drop along the bare tubes. The fin geometric parameters were varied with the ratio of longitudinal fin length to tube diameter (L/D) = 0.50-1.50 [47]; studying the influence of front air conditions and tube wall temperature on the thermohydraulic performance of the heat exchanger bare tube bank and regular finned by varying the air speed 5–20 m/s by simulation. It turns out that the heat transfer coefficient and pressure drop are strongly influenced by the frontal air condition [99]. Study the air side friction equation and heat transfer characteristics for bare tube bank air heat exchanger coolers with variations in tube diameter of 0.5-2 mm and pitch ratio of 1.2 - 4.0 and air velocity from 0.5 - 7.0 m/s in simulation. It turns out that the predictions of the friction equation are more than 80% correlated based on experimental data sources [100]. Based on various studies on staggered bare tube heat exchangers, there is no information regarding the application of staggered bare tube bank heat exchangers as initial air heaters for seaweed convective dryers.

Although there is a lot of research on the thermal performance of bare staggered tube bank heat exchangers, which correlates with the convection coefficient and total heat transfer, there is not much information regarding the study of the total heat transfer of bare staggered tube bank heat exchangers as a waste heat recovery system. The innovation implemented in this research is the introduction of a bare staggered tube bank heat exchanger as a convective dryer waste heat recovery. For this reason, the main focus of this research is the introduction of a bare staggered tube bank heat exchanger by varying the air velocity from 0.5 to 2.5 m/s at the longitudinal pitch ratio (S_L/D) and transverse pitch ratio (S_T/D) specific, which indicates that the heat transfer of the bare staggered tube bank heat exchanger will be further accelerated. This research study is theoretically based on experimental data by examining the average convection coefficient, which will lead to calculating the total heat transfer of the heat exchanger. This research aims to obtain the effective air velocity at which the thermal performance and exit air temperature of the staggered bare tube bank heat exchanger are maximum.

2. MATERIALS AND METHODS

2.1. Experimental equipment and setup

As an initial air heater for seaweed convective dryers, the staggered bare tube heat exchanger consists of two parts, namely the shell and the staggered bare tube bank, the fabrication of which is presented in Figure 1. This research has designed a staggered bare tube heat exchanger as an initial air heater for seaweed convective dryers by considering simulation results using Ansys software.

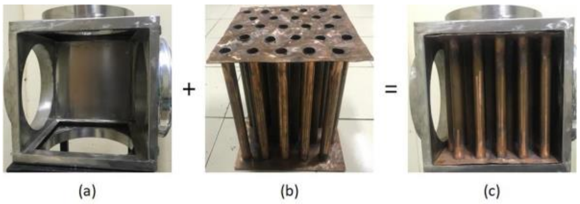

Figure 1. Fabrication steps of bare staggered shell and tube bank; (a) shell, (b) staggered bare tube bank, (c) final assembly of shell and staggered bare tube bank.

Heat transfer to or from a bank (or Bundles) of tubes in crossflow is relevant to various industrial applications. Its geometric arrangement is shown schematically in Figure 2. Typically, one fluid moves through the tube while a second fluid of a different temperature passes through the tube. In this section, a convection heat transfer mechanism occurs, which is related to cross-flow through the pipe.

The rows of tubes in the bank can be staggered in the direction of the fluid velocity as shown in Figure 3. This configuration is characterized by tube diameter (D), transverse pitch distance (S_T), longitudinal pitch distance (S_L), and diagonal pitch distance (S_D) measured between tube centers.

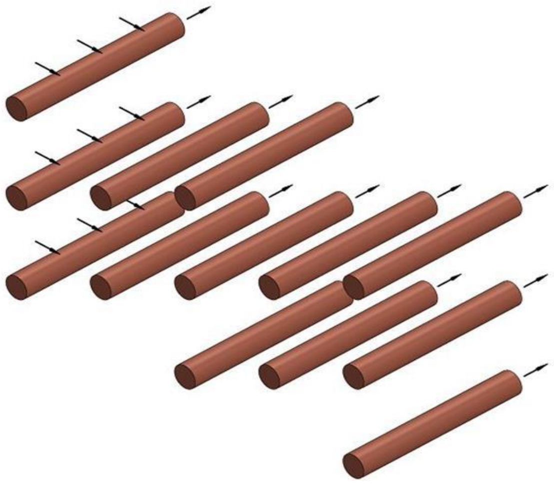

Figure 2. Schematic of a tube bank in cross flow

Display the geometric parameters of the staggered bare tube heat exchanger as an initial air heater for application in seaweed convective dryers. In total, the geometric characteristics of the staggered bare tube heat exchanger are presented in Table 1.

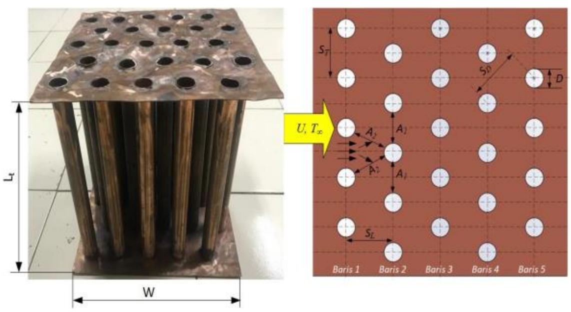

Figure 3. Geometric parameters of heat exchanger tube bank bare staggered

The heat exchanger shell component is made of G.304 stainless steel and has a heat conductivity value of 14.9 W/m.K. The heat exchanger shell wall consists of an adiabatic wall and an isothermal wall. The adiabatic walls are covered with asbestos tape insulation 0.17 m thick between the inner and outer stainless steel. The tube bank heat exchanger component is pure copper with a heat conductivity value of 401 W/m.K.

Table 1. Geometric characteristics of the staggered bare tube heat exchanger.

Parameters	Value (m)
Longitudinal pitch distance (S_L)	0,051
Transverse pitch distance (S_T)	0,051
Diagonal pitch distance (S_D)	0,057
Tube diameter (D_T)	0,0254
Tube length (L_T)	0,030
Tube bank width (W)	0,030
Channel diameter (D_{ch})	0,0282
Inner shell height ($H_{sh,i}$)	0,035
Outer shell height ($H_{sh,o}$)	0,038
Gap distance (G_s)	0,0023
Inner shell width ($B_{sh,i}$)	0,035
Outer shell width ($B_{sh,o}$)	0,038

Supporting components for operating a staggered bare tube heat exchanger are; sauna heater, mini centrifugal blower type MC.DE.125, temperature data logger and control box. To regulate the blower rotation using PWM which is connected to the TX4S-14s temperature control and reading the rotation (rpm) using a tachometer located in the control box. Likewise, the heat input is regulated using PWM to regulate the electric current so that the output power is as desired. 16 channel thermocouple data loggers with a tolerance of ± 1 °C, to measure the temperature of the drying media on; inlet, outlet of tube bank heat exchanger. All temperature measurements use a K-type thermocouple connected to a 16 channels temperature data logger. Calibrate the thermocouple at a water temperature of 100 °C. Hot wire anemometer with a tolerance of ± 3% ± 0.1 digits, to measure the air velocity of hot fluid and cold fluid entering and leaving the heat exchanger. Recording of measured data in the form of temperature, speed, humidity and heat input begins when operating conditions reach steady state.

2.2. Research procedure

A schematic diagram of the research procedure is presented in Figure 4. In this research, the hot fluid and cold fluid cycles occur simultaneously. Hot fluid is air heated by the heater, and cold fluid is air.

The experiment began by setting the heater power to 400 W, the air velocity to 0.5 m/s, and the hot fluid inlet temperature to 50 °C on the box controller. The cold fluid circulating outside the tube will flow into the blower, then through the heater, where the cold fluid will be heated to become hot fluid, reaching 50 C before entering the inlet of the test section. If the temperature exceeds 50 °C, the heater will automatically be disconnected from electricity, and vice versa. If steady conditions have been reached, the process of collecting measured data in temperature and speed begins.

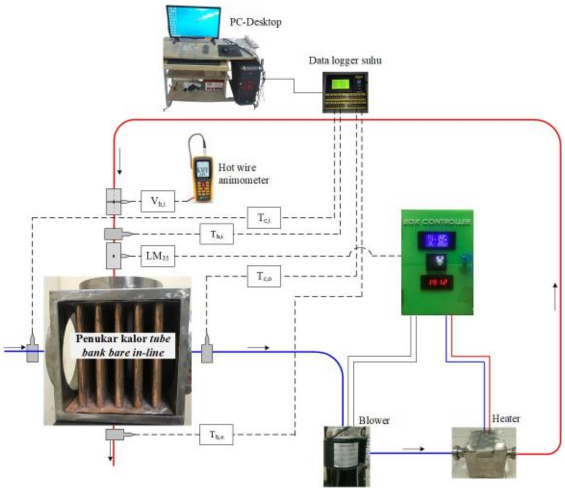

Figure 4. Schematic diagram of research procedures

The test section is provided with a staggered bare tube heat exchanger as an initial air heater with several columns of 5 and several rows of 5. A 0.025 KW centrifugal blower with an air handling capacity of 135 cubic meters per hour is used to supply air as a working fluid at a temperature of 50 °C. The airflow speed is measured with a hot wire anemometer before entering the test section (staggered bare tube heat exchanger). The transverse and longitudinal pitch distance ratio is kept constant for all selected free-air speed settings.

The test section (staggered bare tube heat exchanger) was designed and fabricated to perform several experiments to investigate the heat transfer parameters within the range of operational parameters presented in Table 2.

Schematic diagram of the research procedure with the layout of the LM35 temperature sensor and GM8903 speed sensor, as follows:

1) Measure the temperature of the hot fluid at the inlet and outlet of the heat exchanger (namely, $T_{h,i}$ and $T_{h,o}$).
2) Measurement of the temperature of the cold fluid entering and leaving the heat exchanger (i.e., $T_{c,i}$ and $T_{c,o}$).
3) Air velocity measurement at the heat exchanger inlet (i.e., $V_{h,i}$).

The results of recording measured data will be stored on the anemometer memory card and temperature data logger which is connected automatically to the Desktop PC. Measured data collection was carried out for ± 1 hour until the temperature of the cold fluid leaving the test section had reached a constant condition.

Table 2. Operational parameter range of staggered bare tube heat exchanger.

Parameters	**Range**
P_h, (W)	400
u_∞, (m/s)	0.5, 1, 1.5, 2, 2.5
$T_{h,i}$, (K)	323
D_T, (m)	0,0254
N_T	5
N_L	5
L_T, (m)	0,3
S_L, (m)	0,051
S_T, (m)	0,051
S_D, (m)	0,057

2.3. Data Reduction

Based on Figure 5, presents a schematic illustration of the staggered bare tube heat exchanger research procedure. If it is assumed that the heat exchanger operates at a steady state, where potential energy, conduction, and radiation heat transfer are neglected. To obtain heat exchanger heat transfer, the reduction equation is described as follows:

2.3.1. Maximum air velocity of tube bank

In the case of a staggered bare tube bank heat exchanger as an initial air heater, the free flow velocity of the cold fluid (u) at the inlet is measured with a hot wire anemometer. Maximum air speed can occur in the transverse plane (A_T) or the diagonal plane (A_D), presented in Figure 5.

To determine the maximum air speed occurring in the transverse or diagonal plane, an evaluation of the maximum air speed is carried out using equation (1), which is obtained from [101]:

$$S_D = \left[S_L^2 + \left(\frac{S_T}{2} \right)^2 \right]^{1/2} < \left(\frac{S_T + D}{2} \right) \qquad (1)$$

If the staggered bare tube bank heat exchanger satisfies the inequality above, then the maximum speed occurs in the diagonal plane (A_D). Therefore, the maximum speed in the diagonal plane can be previously estimated using equation (2), which is quoted from [47]:

$$V_{\max} = \frac{2(S_D - D)U_\infty}{S_T} \tag{2}$$

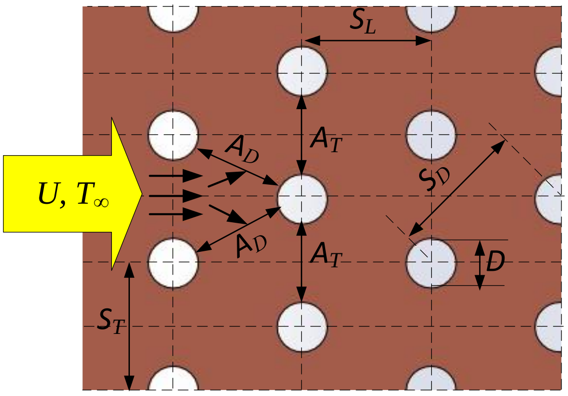

Figure 5. Sketch diagram of maximum air velocity in a staggered bare tube heat exchanger.

On the other hand, bare staggered tube banks do not satisfy the inequality above, so the maximum speed occurs in the transverse plane (A_T), so the maximum air speed in the transverse plane is estimated using equation (3), which is quoted from [58, 102]:

$$V_{\max} = \frac{S_T \cdot U_\infty}{(S_T - D)} \tag{3}$$

2.3.2. Maximum Renolds number of tube bank

In the case of a staggered bare tube bank heat exchanger as an initial air heater where, the Reynolds number for air crossing the tube bank is calculated based on the maximum speed and equivalent hydraulic diameter using equation (4), which is obtained from [103]:

$$\mathrm{Re}_{\max} = \frac{\rho \cdot V_{\max} \cdot D_h}{\mu} \tag{4}$$

2.3.3. Tube bank average Nusselt number

The Nusselt number represents a measure of convection heat transfer compared to conductive heat transfer, which is evaluated based on the Zukauskas correlation using equation (5), which is obtained from [104]:

$$\overline{Nu}_D = C_2 \cdot C_1 \cdot \mathrm{Re}_{D,\max}^{m} \cdot \mathrm{Pr}^{0,36} \left(\frac{\mathrm{Pr}}{\mathrm{Pr}_s}\right)^{1/4} \tag{5}$$

For the range of Reynolds numbers considered in this study, the exponent value m is 0.60 [105]. The value of the constant C_1 varies depending on the tube bank arrangement. The magnitude is $0,35(S_T/S_L)^{1/5} = 0,07$ for the tube bank arrangement considered in this study. Equation (5) applies to tube banks where the number of rows is not more than 20. If the number of rows is less than 20, the correction factor C_2 must be included in the calculation. The C_2 value for five rows of tube banks is 0.92 [47].

2.3.4. Tube bank average convection coefficient

The average convection heat transfer coefficient for the air flow across the staggered bare tube bank is calculated using equation (6), which is obtained from [106]:

$$\bar{h} = \frac{\overline{Nu}_D \cdot k}{D_T} \tag{6}$$

2.3.5. Tube bank logarithmic mean temperature difference

The temperature distribution in the flow in the staggered bare tube bank heat exchanger is not uniform, so it is necessary to use the logarithmic average temperature difference, calculated using equation (7), which is quoted from [78, 107, 108]:

$$\Delta T_{lm} = \frac{(T_s - T_i) - (T_s - T_o)}{\ln\left(\dfrac{T_s - T_i}{T_s - T_o}\right)} \tag{7}$$

where T_o is the exit air temperature of the staggered bare tube bank heat exchanger (K) which can be calculated using equation (8), which is quoted from [104]:

$$T_o = T_s - (T_s - T_i)\exp\left(-\frac{\pi D N \bar{h}_m}{\rho U_\infty N_T S_T c_p}\right) \tag{8}$$

2.3.6. Total tube bank heat transfer

The total heat transfer from the staggered bare tube bank heat exchanger depends on the average heat transfer coefficient, the total heat transfer surface area, and the logarithmic average temperature difference of the tube bank, calculated using equation (9), which is quoted from [109]:

$$Q_{tot} = \bar{h} \cdot \left(N\pi DL_T \right) \Delta T_{lm} \tag{9}$$

3. RESULTS AND DISCUSSION

The results of experimental research on the staggered bare tube bank heat exchanger as an initial air heater carried out based on research procedures and Table 2, range of operational parameters, obtained measured data in the form of free air velocity and temperature, which are presented in Table 3.

Based on Table 3, an analytical study was carried out to examine the thermal performance of the staggered bare tube bank heat exchanger which will be described based on cross flow.

Table 3. Experimentally measured data of staggered bare tube bank heat exchanger.

Q*: 400 W; D: 0,0254 m; N_T: 5; N_L: 5; L: 0,3 m; S_L: 0,051 m; S_T: 0,051; S_D: 0,057; C_1: 0,27; C_2: 0,92; m: 0,63.

Parameters	Range				
u (m/s)	0,5	1,0	1,5	2,0	2,5
T_i (K)	301,7	301,5	301,3	301,1	301,0
T_o (K)	303,6	303,3	302,7	302,5	302,4
$T_{s,1}$ (K)	318,5	317,9	317,6	317,3	317,1
$T_{s,2}$ (K)	318,4	318,1	317,8	317,5	317,2

3.1. Maximum air speed and Reynolds number of tube bank

This section explains the behavior of the maximum air velocity curve in the minimum transverse (A_T) plane and the maximum Reynolds number in a staggered bare tube bank heat exchanger illustrated in Figure 6.

As can be seen in the figure 6, as the air velocity increases, the maximum air speed increases by 20%. This is caused by the increasing free air speed, where the free air speed is directly proportional to the maximum air velocity. The maximum air speed at a free air speed of 2.5 m/s is 4.981 m/s, and the minimum at a free air speed of 0.5 m/s is 0.997 m/s.

Likewise, the greater the free air velocity, the more the Reynolds number increases by 19.90%. This is caused by increased maximum air speed, where maximum air speed is directly proportional to the Reynolds number. The maximum Reynolds number obtained at a free air speed of 2.5 m/s is 788.59, and the minimum Reynolds number obtained at a free air speed of 0.5 m/s is 156.91.

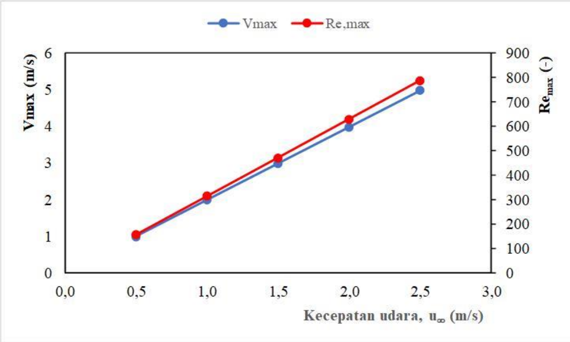

Figure 6. The behavior of air velocity and maximum Reynolds number curves of a staggered bare tube bank heat exchanger.

3.2. Average Nusselt number and convection coefficient tube bank

This section explains the behavior of the Nusselt number and the average convection coefficient curves in the staggered bare tube bank heat exchanger illustrated in Figure 7.

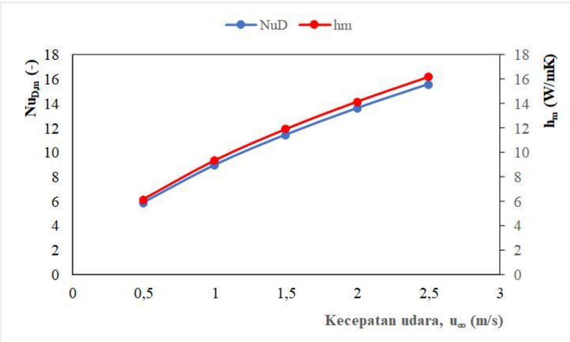

Figure 7. The behaviour of the Nusselt number and average convection coefficient curves of a staggered bare tube bank heat exchanger.

As shown in Figure 7, the average Nusselt number increases by 37.95% as the air velocity increases. This is because the maximum air speed increases, resulting in the Reynolds number growing so that the Nusselt number increases where the Reynolds number is directly proportional to the average Nusselt number. The maximum average Nusselt number is at a free air speed of 2.5 m/s of 15.56, and the minimum is at a free air speed of 0.5 m/s of 5.91.

Likewise, the greater the free air velocity, the greater the average convection coefficient of 38.05%. This is caused by the increasing average Nusselt number, where the average convection coefficient is directly proportional to the Nusselt number. The maximum average convection coefficient is found at a free air speed of 2.5 m/s of 16.19 W/m^2K, and the minimum is found at a free air speed of 0.5 m/s of 6.16 W/m^{2}K.

3.3. Total heat transfer, the temperature of the cold and hot fluid leaving the tube bank

This section explains the behavior of the total number of heat transfer and the exit air temperature in the staggered bare tube bank heat exchanger curves, which is illustrated in Figure 8.

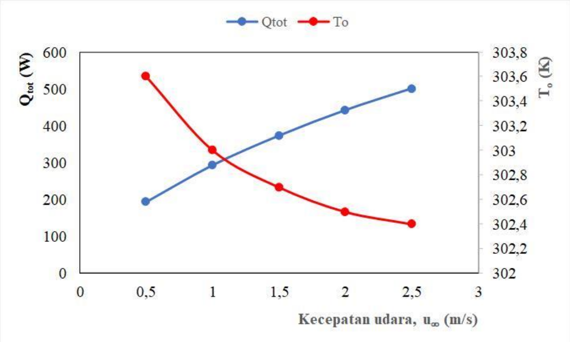

Figure 8. The behaviour of the total heat transfer and air temperature leaving curves of a staggered bare tube bank heat exchanger.

It can be seen in the figure 8 that the greater the air speed, the total heat transfer increases by 38.77%. This is caused by the increasing average convection coefficient resulting in the total heat transfer also increasing where the total heat transfer is directly proportional to the average convection coefficient. The maximum total heat transfer is found at a free air speed of 2.5 m/s of 500.02 W and a minimum at a free air speed of 0.5 m/s of 193.85 W.

On the other hand, the greater the free air velocity, the lower the exit air temperature of the staggered bare tube bank heat exchanger by 99.60%. This is caused by the decreasing temperature gradient between the tube surface temperature and the inlet air temperature of the staggered bare tube bank heat exchanger, where the temperature gradient between the tube surface temperature and the inlet air temperature is directly proportional to the outlet air temperature. The maximum exit air temperature is at a free air speed of 0.5 m/s at 303.6 K and the minimum at 2.5 m/s at 302.4 K..

4. CONCLUSION

The results of experimental research on the thermal performance of a staggered bare tube bank heat exchanger by varying the free air velocity are concluded as follows:

1. The effective free air velocity is at 2.5 m/s, and thermal performance increases by 38.77%.
2. The greater the free air speed, the more the exit air temperature will decrease by 99.60%, where the maximum exit air temperature is at a free air speed of 2.5 m/s of 303.6 K or an increase of 1.9 degrees. This means contributing to savings in electrical energy consumption.

LIST OF NOTATIONS

A_T	Transverse throat width of the tube bank (m^2)
$B_{sh,i}$	Inner shell width (m)
$B_{sh,o}$	Outer shell width (m)
C_1	Constanta
C_2	Correction factor
D_{ch}	Channel diameter (m)
D_T	Tube diameter (m)
G_s	The gap distance between the shell and tube bank (m)
$H_{sh,i}$	Inner shell height (m)
$H_{sh,o}$	Outer shell height (m)
h_m	Average convection coefficient (W/m^{2}K)
$\bar{h}$	Average convection coefficient (W/m^{2}K)
k	Fluid thermal conductivity (W/m.K)
L_T	Tube length (m)
m	Exponent
Nu	Nusselt numbers
$Nu_{,Dm}$	The average Nusselt number
$\overline{Nu}_D$	The average Nusselt number
N_T	Number of rows of tubes in the transverse direction.
N_L	Number of rows of tubes in the longitudinal direction.
P_h	Heater power (W)
Pr	Prandtl numbers
Pr_s	Prandtl number near the wall surface.
Q_{tot}	Total heat transfer (W)
Re	Reynolds Number
Re_{max}	Maximum Reynolds number
S_D	Diagonal tube spacing (m)
S_L	Longitudinal tube spacing (m)
S_T	Transverse tube spacing (m)
T_{hi}	Hot fluid inlet temperature (K)
T_i	Air temperature entering the tube bank (K)
T_o	Air temperature leaving the tube bank (K)
T_s	Tube surface temperature (K)

U_∞	Free flow velocity of air at the entrance of the tube bank (m/s)
V_{max}	Maximum fluid velocity in the tube bank (m/s)
W	Bank tube width (m)
ΔT_{lm}	Logarithmic mean temperature gradient (K)
ρ	Air density (kg/m^3)
μ	Dynamic viscosity of fluids (N-s/m^2)
ν	Fluid kinematic viscosity (m^2/s)

REFERENCES

[1] A. García-Olivares, J. Solé, and O. Osychenko, "Transportation in a 100% renewable energy system," *Energy Convers. Manag.*, vol. 158, no. August 2017, pp. 266–285, 2018, doi: 10.1016/j.enconman.2017.12.053.

[2] D. Gielen, F. Boshell, D. Saygin, M. D. Bazilian, N. Wagner, and R. Gorini, "The role of renewable energy in the global energy transformation," *Energy Strateg. Rev.*, vol. 24, no. June 2018, pp. 38–50, 2019, doi: 10.1016/j.esr.2019.01.006.

[3] D. A. Cullen *et al.*, "New roads and challenges for fuel cells in heavy-duty transportation," *Nat. Energy*, vol. 6, no. 5, pp. 462–474, 2021, doi: 10.1038/s41560-021-00775-z.

[4] S. Griffiths, D. Furszyfer Del Rio, and B. Sovacool, "Policy mixes to achieve sustainable mobility after the COVID-19 crisis," *Renew. Sustain. Energy Rev.*, vol. 143, no. February, p. 110919, 2021, doi: 10.1016/j.rser.2021.110919.

[5] V. Chan, A. Davies, L. Wellard-Cole, and M. Allman-Farinelli, "The energy density of meals and snacks consumed by young Australian adults (18-30 years old) are influenced by preparation location but not screen use nor social interactions: findings from the MYMeals wearable camera study," *J. Nutr. Sci.*, vol. 11, no. 5, pp. 1–11, 2022, doi: 10.1017/jns.2022.76.

[6] M. A. Alkhadra *et al.*, "Electrochemical Methods for Water Purification, Ion Separations, and Energy Conversion," *Chem. Rev.*, vol. 122, no. 16, pp. 13547–13635, 2022, doi: 10.1021/acs.chemrev.1c00396.

[7] R. Krishnamoorthy, I. D. Soubache, and S. Jain, "Wireless Communication Based Evaluation of Power Consumption for Constrained Energy System," *Wirel. Pers. Commun.*, vol. 127, no. 1, pp. 737–748, 2022, doi: 10.1007/s11277-021-08402-6.

[8] G. Kalt, D. Wiedenhofer, C. Görg, and H. Haberl, "Conceptualizing energy services: A review of energy and well-being along the Energy Service Cascade," *Energy Res. Soc. Sci.*, vol. 53, no. November 2018, pp. 47–58, 2019, doi: 10.1016/j.erss.2019.02.026.

[9] M. Farghali *et al.*, *Strategies to save energy in the context of the energy crisis: a review*, vol. 21, no. 4. Springer International Publishing, 2023. doi: 10.1007/s10311-023-01591-5.

[10] J. Johannesson and D. Clowes, "Energy Resources and Markets - Perspectives on the Russia-Ukraine War," *Eur. Rev.*, vol. 30, no. 1, pp. 4–23, 2022, doi: 10.1017/S1062798720001040.

[11] G. B. de Campos, C. Bringhenti, A. Traverso, and J. T. Tomita, "Thermoeconomic optimization of organic Rankine bottoming cycles for micro gas turbines," *Appl. Therm. Eng.*, vol. 164, p. 114477, 2020, doi: 10.1016/j.applthermaleng.2019.114477.

[12] Y. W. Huang, M. Q. Chen, and L. Jia, "Assessment on thermal behavior of municipal sewage sludge thin-layer during hot air forced convective drying," *Appl. Therm. Eng.*, vol. 96, pp. 209–216, Mar. 2016, doi: 10.1016/j.applthermaleng.2015.11.090.

[13] R. Moreira, F. Chenlo, J. Sineiro, S. Arufe, and S. Sexto, "Water Sorption Isotherms and Air Drying Kinetics of Fucus vesiculosus Brown Seaweed," *J. Food Process. Preserv.*, vol. 41, no. 4, Aug. 2017, doi: 10.1111/jfpp.12997.

[14] M. Stramarkou, S. Papadaki, K. Kyriakopoulou, and M. Krokida, "Effect of drying and extraction conditions on the recovery of bioactive compounds from Chlorella vulgaris," *J. Appl. Phycol.*, vol. 29, no. 6, pp. 2947–2960, 2017, doi: 10.1007/s10811-017-1181-8.

[15] S. Kazemi, M. I. M. Nor, and W. H. Teoh, "Thermodynamic and economic investigation of an ionic liquid as a new proposed geothermal fluid in different organic Rankine cycles for energy production," *Energy*, vol. 193, p. 116722, 2020, doi: 10.1016/j.energy.2019.116722.

[16] M. H. Masud, A. A. Ananno, A. M. E. Arefin, R. Ahamed, P. Das, and M. U. H. Joardder, "Perspective of biomass energy conversion in Bangladesh," *Clean Technologies and Environmental Policy*, vol. 21, no. 4. Springer Verlag, pp. 719–731, May 15, 2019. doi: 10.1007/s10098-019-01668-2.

[17] Z. Su *et al.*, "Green and efficient configuration of integrated waste heat and cold energy recovery for marine natural gas/diesel dual-fuel engine," *Energy Convers. Manag.*, vol. 209, no. March, 2020, doi: 10.1016/j.enconman.2020.112650.

[18] E. Blanco-Davis and P. Zhou, "Life Cycle Assessment as a complementary utility to regulatory measures of shipping energy efficiency," *Ocean Eng.*, vol. 128, no. September 2015, pp. 94–104, 2016, doi: 10.1016/j.oceaneng.2016.10.015.

[19] A. Akbari, S. Kouravand, and G. Chegini, "Experimental analysis of a rotary heat exchanger for waste heat recovery from the exhaust gas of dryer," *Appl. Therm. Eng.*, vol. 138, pp. 668–674, Jun. 2018, doi: 10.1016/j.applthermaleng.2018.04.103.

[20] S. M. Shalaby, M. A. Bek, and A. E. Kabeel, "Design Recommendations for Humidification-dehumidification Solar Water Desalination Systems," in *Energy Procedia*, Elsevier Ltd, Feb. 2017, pp. 270–274. doi: 10.1016/j.egypro.2016.12.148.

[21] A. E. Kabeel, M. Abdelgaied, and A. Eisa, "Enhancing the performance of single basin solar still using high thermal conductivity sensible storage materials," *J. Clean. Prod.*, vol. 183, pp. 20–25, May 2018, doi: 10.1016/j.jclepro.2018.02.144.

[22] N. Titahelu, C. S. E. Tupamahu, and S. J. E. Sarwuna, "Evaluasi Kinerja Pelat Kolektor Datar Dengan Berbagai Model Tube Kolektor Sebagai Pemanas Air Surya Aktif," *ALE Proceeding*, vol. 5, pp. 53–58, 2022, doi: 10.30598/ale.5.2022.53-58.

[23] N. S. F. Syatauw, A. Simanjuntak, and N. Titahelu, "Analisis kinerja panel surya akibat pendinginan aktif," *Isometri*, vol. 2, no. 1, 2023.

[24] M. Yahya, A. Fudholi, and K. Sopian, "Energy and exergy analyses of solar-assisted fluidized bed drying integrated with biomass furnace," *Renew. Energy*, vol. 105, pp. 22–29, 2017, doi: 10.1016/j.renene.2016.12.049.

[25] Hamdani, T. A. Rizal, and Z. Muhammad, "Fabrication and testing of hybrid solar-biomass dryer for drying fish," *Case Stud. Therm. Eng.*, vol. 12, pp. 489–496, Sep. 2018, doi: 10.1016/j.csite.2018.06.008.

[26] M. C. Ndukwu, M. Simo-Tagne, F. I. Abam, O. S. Onwuka, S. Prince, and L. Bennamoun, "Exergetic sustainability and economic analysis of hybrid solar-biomass dryer integrated with copper tubing as heat exchanger," *Heliyon*, vol. 6, no. 2, Feb. 2020, doi: 10.1016/j.heliyon.2020.e03401.

[27] I. B. Alit, I. G. B. Susana, and I. M. Mara, "Utilization of rice husk biomass in the conventional corn dryer based on the heat exchanger pipes diameter," *Case Stud. Therm. Eng.*, vol. 22, Dec. 2020, doi: 10.1016/j.csite.2020.100764.

[28] N. Badshah, K. A. Al-attab, and Z. A. Zainal, "Design optimization and experimental analysis of externally fired gas turbine system fuelled by biomass," *Energy*, vol. 198, 2020, doi: 10.1016/j.energy.2020.117340.

[29] W. M. Rumaherang, B. Laconawa, N. Titahelu, and J. Louhenapessy, "Kajian Perbandingan Performance Energi Turbin Angin Model Ducted Dengan Un-Ducted," *J. Tek. Mesin, Elektro, Inform. Kelaut. dan Sains*, vol. 2, no. 1, pp. 56–64, 2022, doi: 10.30598/metiks.2022.2.1.56-64.

[30] N. Jamshidi and A. Mosaffa, "Investigating the effects of geometric parameters on finned conical helical geothermal heat exchanger and its energy extraction capability," *Geothermics*, vol. 76, pp. 177–189, Nov. 2018, doi: 10.1016/j.geothermics.2018.07.007.

[31] A. Keshvarparast, S. S. M. Ajarostaghi, and M. A. Delavar, "Thermodynamic analysis the performance of hybrid solar-geothermal power plant equipped with air-cooled condenser," *Appl. Therm. Eng.*, vol. 172, May 2020, doi: 10.1016/j.applthermaleng.2020.115160.

[32] F. Esmaeilion, "Hybrid renewable energy systems for desalination," *Appl. Water Sci.*, vol. 10, no. 3, Mar. 2020, doi: 10.1007/s13201-020-1168-5.

[33] W. M. Rumaherang and J. Latuny, "Fluid Flow Study in Various Shapes and Sizes of

Horizontal Axis Sea Current Turbine," *Sinergi*, vol. 25, no. 3, p. 289, 2021, doi: 10.22441/sinergi.2021.3.006.

[34] M. W. Kareem, S. I. Gilani, K. Habib, K. Irshad, and B. B. Saha, "Performance analysis of a multi-pass solar thermal collector system under transient state assisted by porous media," *Sol. Energy*, vol. 158, pp. 782–791, Dec. 2017, doi: 10.1016/j.solener.2017.10.016.

[35] J. Li, Z. Yang, S. Hu, F. Yang, and Y. Duan, "Effects of shell-and-tube heat exchanger arranged forms on the thermo-economic performance of organic Rankine cycle systems using hydrocarbons," *Energy Convers. Manag.*, vol. 203, Jan. 2020, doi: 10.1016/j.enconman.2019.112248.

[36] S. A. Nada, R. Khater, and M. A. Mahmoud, "Thermal characteristics enhancement of helical cooling-dehumidifying coils using strips fins," *Therm. Sci. Eng. Prog.*, vol. 16, May 2020, doi: 10.1016/j.tsep.2020.100482.

[37] Z. Mat Nawi, S. K. Kamarudin, S. R. Sheikh Abdullah, and S. S. Lam, "The potential of exhaust waste heat recovery (WHR) from marine diesel engines via organic rankine cycle," *Energy*, vol. 166, pp. 17–31, 2019, doi: 10.1016/j.energy.2018.10.064.

[38] M. C. Rajagopal *et al.*, "Materials-to-device design of hybrid metal-polymer heat exchanger tubes for low temperature waste heat recovery," *Int. J. Heat Mass Transf.*, vol. 143, Nov. 2019, doi: 10.1016/j.ijheatmasstransfer.2019.118497.

[39] X. Han, H. Zou, J. Wu, C. Tian, M. Tang, and G. Huang, "Investigation on the heating performance of the heat pump with waste heat recovery for the electric bus," *Renew. Energy*, vol. 152, pp. 835–848, Jun. 2020, doi: 10.1016/j.renene.2020.01.075.

[40] A. Singh, J. Sarkar, and R. R. Sahoo, "Experiment on waste heat recovery-assisted heat pump drying of food chips: Performance, economic, and exergoeconomic analyses," *J. Food Process. Preserv.*, vol. 44, no. 9, Sep. 2020, doi: 10.1111/jfpp.14699.

[41] G. V. Ochoa, J. P. Rojas, and J. D. Forero, "Advance Exergo-economic analysis of a waste heat recovery system using ORC for a bottoming natural gas engine," *Energies*, vol. 13, no. 1, 2020, doi: 10.3390/en13010267.

[42] Z. Cheng, Z. Tan, Z. Guo, J. Yang, and Q. Wang, "Technologies and fundamentals of waste heat recovery from high-temperature solid granular materials," *Applied Thermal Engineering*, vol. 179. Elsevier Ltd, Oct. 01, 2020. doi: 10.1016/j.applthermaleng.2020.115703.

[43] O. Chibuike, D. N. Olisaemeka Chukwudozie, D. N. Nnaemeka Reginald, D. O. Chukwunenye Anthony, D. I. Onyechege Johnson, and P. E. Enyioma Anyanwu, "Energy Consumption of Yam Slice Drying in an Exhaust Gas Waste Heat Recovery Hot Air Tray Dryer," *Sci. Res. J.*, vol. 9, no. 8, pp. 1–7, Aug. 2021, doi: 10.31364/scirj/v9.i08.2021.p0821872.

[44] Z. Su *et al.*, "Opportunities and strategies for multigrade waste heat utilization in various industries: A recent review," *Energy Convers. Manag.*, vol. 229, no. January, p. 113769, 2021, doi: 10.1016/j.enconman.2020.113769.

[45] S. Lion, C. N. Michos, I. Vlaskos, C. Rouaud, and R. Taccani, "A review of waste heat recovery and Organic Rankine Cycles (ORC) in on-off highway vehicle Heavy Duty Diesel Engine applications," *Renew. Sustain. Energy Rev.*, vol. 79, no. May, pp. 691–708, 2017, doi: 10.1016/j.rser.2017.05.082.

[46] M. H. Masud, M. U. Joardder, M. Tariqul Islam, M. Munthakimoon Hasan, and M. Muntasir Ahmed, "Feasibility of utilizing waste heat in drying of plant-based food materials Renewable Energy View project Intermittent Microwave convective drying View project Feasibility of utilizing waste heat in drying of plant-based food materials," *Int. Conf. Mech. Ind. Mater. Eng.*, vol. 2017, 2017, [Online]. Available: https://www.researchgate.net/publication/325321933

[47] J. D. Abraham, A. S. Dhoble, and C. K. Mangrulkar, "Numerical analysis for thermo-hydraulic performance of staggered cross flow tube bank with longitudinal tapered fins," *Int. Commun. Heat Mass Transf.*, vol. 118, Nov. 2020, doi:

10.1016/j.icheatmasstransfer.2020.104905.

[48] A. T. Hoang, “Waste heat recovery from diesel engines based on Organic Rankine Cycle,” *Appl. Energy*, vol. 231, no. March, pp. 138–166, 2018, doi: 10.1016/j.apenergy.2018.09.022.

[49] X. Wang, M. Jin, W. Feng, G. Shu, H. Tian, and Y. Liang, “Cascade energy optimization for waste heat recovery in distributed energy systems,” *Appl. Energy*, vol. 230, no. June, pp. 679–695, 2018, doi: 10.1016/j.apenergy.2018.08.124.

[50] A. Mahmoudi, M. Fazli, and M. R. Morad, “A recent review of waste heat recovery by Organic Rankine Cycle,” *Appl. Therm. Eng.*, vol. 143, no. July, pp. 660–675, 2018, doi: 10.1016/j.applthermaleng.2018.07.136.

[51] M. U. H. Joardder and M. H. Masud, “Feasibility of Advance Technologies,” in *Food Preservation in Developing Countries: Challenges and Solutions*, Springer International Publishing, 2019, pp. 219–236. doi: 10.1007/978-3-030-11530-2_9.

[52] A. E. Quintero and M. Vera, “Laminar counterflow parallel-plate heat exchangers: An exact solution including axial and transverse wall conduction effects,” *Int. J. Heat Mass Transf.*, vol. 104, pp. 1229–1245, Jan. 2017, doi: 10.1016/j.ijheatmasstransfer.2016.09.025.

[53] H. Sun *et al.*, “A general distributed-parameter model for thermal performance of cold box with parallel plate-fin heat exchangers based on graph theory,” *Appl. Therm. Eng.*, vol. 148, pp. 478–490, Feb. 2019, doi: 10.1016/j.applthermaleng.2018.11.054.

[54] Y. A. Al-Turki, H. Moria, A. Shawabkeh, S. Pourhedayat, M. Hashemian, and H. S. Dizaji, “Thermal, frictional and exergetic analysis of non-parallel configurations for plate heat exchangers,” *Chem. Eng. Process. - Process Intensif.*, vol. 161, Apr. 2021, doi: 10.1016/j.cep.2021.108319.

[55] R. Eldeeb, V. Aute, and R. Radermacher, “Pillow plate heat exchanger weld shape optimization using approximation and parallel parameterized CFD and non-uniform rational B-splines,” *Int. J. Refrig.*, vol. 110, pp. 121–131, Feb. 2020, doi: 10.1016/j.ijrefrig.2019.10.024.

[56] B. O. Kwon, H. Kim, J. Noh, S. Y. Lee, J. Nam, and J. S. Khim, “Spatiotemporal variability in microphytobenthic primary production across bare intertidal flat, saltmarsh, and mangrove forest of Asia and Australia,” *Mar. Pollut. Bull.*, vol. 151, Feb. 2020, doi: 10.1016/j.marpolbul.2019.110707.

[57] A. M. N. Elmekawy, A. A. Ibrahim, A. M. Shahin, S. Al-Ali, and G. E. Hassan, “Performance enhancement for tube bank staggered configuration heat exchanger – CFD Study,” *Chem. Eng. Process. - Process Intensif.*, vol. 164, Jul. 2021, doi: 10.1016/j.cep.2021.108392.

[58] X. Song, M. Liu, X. Hu, X. Wang, T. Liao, and J. Sun, “Numerical analysis of flow across brush elements based on a 2-D staggered tube banks model,” *Aerospace*, vol. 8, no. 1, pp. 1–16, Jan. 2021, doi: 10.3390/aerospace8010019.

[59] N. Alvandifar *et al.*, “Experimental study of partially metal foam wrapped tube bundles,” *Int. J. Therm. Sci.*, vol. 162, Apr. 2021, doi: 10.1016/j.ijthermalsci.2020.106798.

[60] A. Hashem-ol-Hosseini, M. Akbarpour Ghazani, A. Shahsavari, and M. Soltani, “Experimental investigation of thermal-hydraulic characteristics of finned oval tube bundles in cross-flow arrangements,” *Int. J. Heat Mass Transf.*, vol. 180, Dec. 2021, doi: 10.1016/j.ijheatmasstransfer.2021.121759.

[61] N. Titahelu, B. G. Tentua, and S. A. L. Payapo, “Analisis kinerja termal penukar kalor tube bank bare in-line aliran silang sebagai pemulihan limbah panas pengering konvektif rumput laut,” *J. METIKS*, vol. 3, no. 2, pp. 1–14, 2023, doi: https://doi.org/10.30598/metiks.2023.3.2.1-14.

[62] A. S. Baqir, H. B. Mahood, and A. R. Kareem, “Optimisation and evaluation of NTU and effectiveness of a helical coil tube heat exchanger with air injection,” *Therm. Sci. Eng. Prog.*, vol. 14, Dec. 2019, doi: 10.1016/j.tsep.2019.100420.

[63] Y. Han, X. sheng Wang, Z. Zhang, and H. nan Zhang, “Multi-objective optimization of geometric parameters for the helically coiled tube using Markowitz optimization theory,” *Energy*, vol. 192, Feb. 2020, doi:

10.1016/j.energy.2019.116567.

[64] A. Hatumessen, N. Titahelu, and C. S. Tupamahu, "Analisis efektivitas penukar kalor pipa helikal destilasi minyak atsiri kayu putih," in *Archepelago Engineering*, N. Titahelu, Ed., Amon: Fakultas Teknik Universitas Pattimura, 2021, pp. 127–132. doi: 10.30598/ale.4.2021.127-132.

[65] G. Kumar, Gagandeep, A. Kumar, N. A. Ansari, and M. Zunaid, "Comparative numerical study of flow characteristics in shell & helical coil heat exchangers with hybrid models," in *Materials Today: Proceedings*, Elsevier Ltd, 2021, pp. 10831–10836. doi: 10.1016/j.matpr.2021.01.775.

[66] M. Farnam, M. Khoshvaght-Aliabadi, and M. J. Asadollahzadeh, "Intensified single-phase forced convective heat transfer with helical-twisted tube in coil heat exchangers," *Ann. Nucl. Energy*, vol. 154, May 2021, doi: 10.1016/j.anucene.2020.108108.

[67] N. Titahelu, J. Latuny, C. S. E. Tupamahu, and S. J. E. Sarwuna, "Pitch ratio effect on the effectiveness of condenser for essential oil distillation," *J. Energy, Mech. Mater. Manuf. Eng.*, vol. 6, no. 2, pp. 145–154, doi: https://doi.org/10.22219/jemmme.v6i2.19461.

[68] Y. Yao, Q. Zhu, and Z. Li, "Performance of helically coiled gas heaters in supercritical CO2 Rankine cycles: A detailed assessment under convective boundary condition," *Energy*, vol. 195, Mar. 2020, doi: 10.1016/j.energy.2020.117002.

[69] N. Titahelu, D. S. Pelupessy, C. S. E. Tupamahu, and A. F. Rumagutawan, "Meningkatkan efektivitas kondensor vertikal pipa helikal koil untuk destilasi minyak atsiri sereh," *J. Rekayasa Mesin*, vol. 14, no. 1, pp. 235–249, 2023, doi: 10.21776/jrm.v14i1.1219.

[70] Z. Said, S. M. A. Rahman, M. El Haj Assad, and A. H. Alami, "Heat transfer enhancement and life cycle analysis of a Shell-and-Tube Heat Exchanger using stable CuO/water nanofluid," *Sustain. Energy Technol. Assessments*, vol. 31, pp. 306–317, Feb. 2019, doi: 10.1016/j.seta.2018.12.020.

[71] X. Yang, J. Yu, T. Xiao, Z. Hu, and Y. L. He, "Design and operating evaluation of a finned shell-and-tube thermal energy storage unit filled with metal foam," *Appl. Energy*, vol. 261, no. December 2019, p. 114385, 2020, doi: 10.1016/j.apenergy.2019.114385.

[72] M. Fares, M. AL-Mayyahi, and M. AL-Saad, "Heat transfer analysis of a shell and tube heat exchanger operated with graphene nanofluids," *Case Stud. Therm. Eng.*, vol. 18, p. 100584, 2020, doi: 10.1016/j.csite.2020.100584.

[73] R. Said, N. Titahelu, and R. Ufie, "Analisis laju aliran massa fluida dingin terhadap efektivitas penukar kalor shell and tube destilasi minyak atsiri cengkeh (Syzygium aromaticum)," in *Archipelago Engineering (ALE)*, N. Titahelu, Ed., Ambon: Fakultas Teknik Universitas Pattimura, 2021, pp. 140–145. doi: https://doi.org/10.30598/ale.4.2021.140-145.

[74] E. M. S. El-Said and M. M. A. Alsood, "Experimental investigation of air injection effect on the performance of horizontal shell and multi-tube heat exchanger with baffles," *Appl. Therm. Eng.*, vol. 134, pp. 238–247, Apr. 2018, doi: 10.1016/j.applthermaleng.2018.02.001.

[75] G. Yu, L. Xiong, C. Du, and H. Chen, "Simplified model and performance analysis for top insulated metal ceiling radiant cooling panels with serpentine tube arrangement," *Case Stud. Therm. Eng.*, vol. 11, pp. 35–42, Mar. 2018, doi: 10.1016/j.csite.2017.12.006.

[76] L. Liu *et al.*, "Numerical investigation of mass transfer characteristics for the desiccant-coated dehumidification wheel in a dehumidification process," *Appl. Therm. Eng.*, vol. 160, Sep. 2019, doi: 10.1016/j.applthermaleng.2019.113944.

[77] H. Gürbüz and D. Ateş, "A numerical Study on Processes of Charge and Discharge of Latent Heat Energy Storage System Using RT27 Paraffin Wax for Exhaust Waste Heat Recovery in a SI Engine," *Int. J. Automot. Sci. Technol.*, vol. 4, pp. 314–327, 2020, doi: 10.30939/ijastech..800856.

[78] N. Titahelu, J. Louhenapessy, J. S. Litiloly, and A. Arson, "Studi perbandingan efektivitas berbagai model tube penukar

kalor sebagai sistem pemulihan limbah panas," in *Seminar Nasional "ARCHIPELAGO ENGINEERING,"* N. Titahelu, Ed., Ambon: Fakultas Teknik Universitas Pattimura, 2023, pp. 20–31. doi: 10.30598/ale.6.2023.20-31.

[79] S. Chakrabarty and U. S. Wankhede, "Flow and heat transfer behaviour across circular," *Int. J. Mod. Eng. Res.*, vol. 2, no. 4, pp. 1529–1533, 2012.

[80] J. M. Gorman, E. M. Sparrow, and J. Ahn, "In-line tube-bank heat exchangers: Arrays with various numbers of thermally participating tubes," *Int. J. Heat Mass Transf.*, vol. 132, pp. 837–847, Apr. 2019, doi: 10.1016/j.ijheatmasstransfer.2018.11.167.

[81] S. Kotšmíd and Z. Brodnianská, "Determination of the reference temperature for a convective heat transfer coefficient in a heated tube bank," *Appl. Sci.*, vol. 11, no. 22, 2021, doi: 10.3390/app112210564.

[82] C. K. Mangrulkar, A. S. Dhoble, S. Chamoli, A. Gupta, and V. B. Gawande, "Recent advancement in heat transfer and fluid flow characteristics in cross flow heat exchangers," *Renewable and Sustainable Energy Reviews*, vol. 113. Elsevier Ltd, Oct. 01, 2019. doi: 10.1016/j.rser.2019.06.027.

[83] T. A. Tahseen, M. Ishak, and M. M. Rahman, "An overview on thermal and fluid flow characteristics in a plain plate finned and un-finned tube banks heat exchanger," *Renew. Sustain. Energy Rev.*, vol. 43, pp. 363–380, 2015, doi: 10.1016/j.rser.2014.10.070.

[84] H. Kim Phang, C.-M. Chu, S. Kumaresan, M. Mizanur Rahman, H.-K. Phang, and S. Md Yasir, "Preliminary Study of Seaweed Drying under A Shade and in A Natural Draft Solar Dryer," *Artic. Int. J. Sci. Eng.*, vol. 8, no. 1, pp. 10–14, 2014, doi: 10.12777/ijse.8.1.10-14.

[85] A. M. González, M. Vaz, and P. S. B. Zdanski, "A hybrid numerical-experimental analysis of heat transfer by forced convection in plate-finned heat exchangers," *Appl. Therm. Eng.*, vol. 148, pp. 363–370, Feb. 2019, doi: 10.1016/j.applthermaleng.2018.11.068.

[86] C. K. Mangrulkar, A. S. Dhoble, J. D. Abraham, and S. Chamoli, "Experimental and numerical investigations for effect of longitudinal splitter plate configuration for thermal-hydraulic performance of staggered tube bank," *Int. J. Heat Mass Transf.*, vol. 161, Nov. 2020, doi: 10.1016/j.ijheatmasstransfer.2020.120280.

[87] H. Ghasemkhani, A. Keyhani, M. Aghbashlo, S. Rafiee, and A. S. Mujumdar, "Improving exergetic performance parameters of a rotating-tray air dryer via a simple heat exchanger," *Appl. Therm. Eng.*, vol. 94, pp. 13–23, Feb. 2016, doi: 10.1016/j.applthermaleng.2015.10.114.

[88] A. A. Ananno, M. H. Masud, P. Dabnichki, and A. Ahmed, "Design and numerical analysis of a hybrid geothermal PCM flat plate solar collector dryer for developing countries," *Sol. Energy*, vol. 196, no. April 2019, pp. 270–286, 2020, doi: 10.1016/j.solener.2019.11.069.

[89] Z. Erbay and A. Hepbasli, "Assessment of cost sources and improvement potentials of a ground-source heat pump food drying system through advanced exergoeconomic analysis method," *Energy*, vol. 127, pp. 502–515, 2017, doi: 10.1016/j.energy.2017.03.148.

[90] M. H. Masud, A. A. Ananno, N. Ahmed, P. Dabnichki, and K. N. Salehin, "Experimental investigation of a novel waste heat based food drying system," *J. Food Eng.*, vol. 281, Sep. 2020, doi: 10.1016/j.jfoodeng.2020.110002.

[91] M. Mohanraj, "Performance of a solar-ambient hybrid source heat pump drier for copra drying under hot-humid weather conditions," *Energy Sustain. Dev.*, vol. 23, pp. 165–169, 2014, doi: 10.1016/j.esd.2014.09.001.

[92] M. Hasanuzzaman, A. B. M. A. Malek, M. M. Islam, A. K. Pandey, and N. A. Rahim, "Global advancement of cooling technologies for PV systems: A review," *Sol. Energy*, vol. 137, pp. 25–45, 2016, doi: 10.1016/j.solener.2016.07.010.

[93] M. Hatami, M. Jafaryar, J. Zhou, and D. Jing, "Investigation of engines radiator heat recovery using different shapes of nanoparticles in H2O/(CH2OH)2 based nanofluids," *Int. J. Hydrogen Energy*, vol. 42, no. 16, pp. 10891–10900, Apr. 2017, doi: 10.1016/j.ijhydene.2017.01.196.

[94] R. Saidur, “Energy consumption, energy savings, and emission analysis in Malaysian office buildings,” *Energy Policy*, vol. 37, no. 10, pp. 4104–4113, 2009, doi: 10.1016/j.enpol.2009.04.052.

[95] B. El Fil and S. Garimella, “The state of the art in energy saving techniques for garment/textile drying,” *Dry. Technol.*, vol. 40, no. 11, pp. 2235–2250, 2022, doi: 10.1080/07373937.2021.1938599.

[96] R. T. Oğulata, “Utilization of waste-heat recovery in textile drying,” *Appl. Energy*, vol. 79, no. 1, pp. 41–49, 2004, doi: 10.1016/j.apenergy.2003.12.002.

[97] R. L. S. Mainardes, R. S. Matos, J. V. C. Vargas, and J. C. Ordonez, “Optimally staggered finned circular and elliptic tubes in turbulent forced convection,” *J. Heat Transfer*, vol. 129, no. 5, pp. 674–678, 2007, doi: 10.1115/1.2712860.

[98] R. S. Matos, J. V. C. Vargas, T. A. Laursen, and A. Bejan, “Optimally staggered finned circular and elliptic tubes in forced convection,” *Int. J. Heat Mass Transf.*, vol. 47, no. 6–7, pp. 1347–1359, 2004, doi: 10.1016/j.ijheatmasstransfer.2003.08.015.

[99] L. D. Gu and J. C. Min, “Airside thermal-hydraulic characteristics for tube bank heat exchangers used to cool compressor bleed air in an aero engine,” *Appl. Therm. Eng.*, vol. 141, pp. 939–947, Aug. 2018, doi: 10.1016/j.applthermaleng.2018.06.033.

[100] D. Bacellar, V. Aute, Z. Huang, and R. Radermacher, “Airside friction and heat transfer characteristics for staggered tube bundle in crossflow configuration with diameters from 0.5 mm to 2.0 mm,” *Int. J. Heat Mass Transf.*, vol. 98, pp. 448–454, Jul. 2016, doi: 10.1016/j.ijheatmasstransfer.2016.02.072.

[101] M. Nasif Kuru, M. T. Erdinc, and A. Yilmaz, “Optimization of Heat Transfer and Pressure Drop in Axially Finned Staggered Tube Banks,” *Heat Transf. Eng.*, pp. 1–18, 2020, doi: 10.1080/01457632.2020.1785696.

[102] G. TÜRKAKAR, “Design and Optimization of Pcm-Air Cold Energy Storage Device To Be Used for Peak Electricity Shaving,” *Isı Bilim. ve Tek. Derg.*, vol. 41, no. 1, pp. 23–36, 2021, doi: 10.47480/isibted.979300.

[103] L. Gu, J. Min, X. Wu, and L. Yang, “Airside heat transfer and pressure loss characteristics of bare and finned tube heat exchangers used for aero engine cooling considering variable air properties,” *Int. J. Heat Mass Transf.*, vol. 108, pp. 1839–1849, 2017, doi: 10.1016/j.ijheatmasstransfer.2017.01.047.

[104] W. A. Khan, J. R. Culham, and M. M. Yovanovich, “Convection heat transfer from tube banks in crossflow: Analytical approach,” *Int. J. Heat Mass Transf.*, vol. 49, no. 25–26, pp. 4831–4838, Dec. 2006, doi: 10.1016/j.ijheatmasstransfer.2006.05.042.

[105] T. L. Bergman, A. S. Lavine, F. P. Incropera, and D. P. DeWitt, *Fundamentals of Heat and Mass Transfer*, vol. 21, no. 1. John Wiley and Sons Inc, 2011.

[106] A. Banasode, S. Valmiki, and V. S. Desai, “Design and Analysis of Bagasse Dryer to Recover Energy of Water Tube Boiler in a Sugar Factory,” *Int. J. Innov. Technol. Res.*, vol. 5, no. 4, pp. 6645–6652, 2017.

[107] B. Lotfi and B. Sundén, “Development of new finned tube heat exchanger: Innovative tube-bank design and thermohydraulic performance,” *Heat Transf. Eng.*, vol. 41, no. 14, pp. 1209–1231, Aug. 2020, doi: 10.1080/01457632.2019.1637112.

[108] D. Mondal, M. O. Ikram, M. F. Rabbi, and M. N. A. Moral, “Experimental Investigation and Comparison of Bend Tube Parallel & Counter Flow and Cross Flow Water to Air Heat Exchanger,” *Int. J. Sci. Eng. Res.*, vol. 5, no. 7, pp. 686–695, 2014.

[109] S. Sahamifar, F. Kowsary, and M. H. Mazlaghani, “Generalized optimization of cross-flow staggered tube banks using a subscale model,” *Int. Commun. Heat Mass Transf.*, vol. 105, pp. 46–57, Jun. 2019, doi: 10.1016/j.icheatmasstransfer.2019.03.004.